Optical-potential study of electron-hydrogen scattering at intermediate energies

J. Callaway and K. Unnikrishnan
Department of Physics and Astronomy, Louisana State University, Baton Rouge, Louisiana 70803-4001

D. H. Oza
National Bureau of Standards, Gaithersburg, Maryland 20899
(Received 4 May 1987)

Electron-hydrogen scattering is studied in the range of incident energies from 12 to 100 eV. The equations resulting from a six-state close-coupling expansion are supplemented by an optical potential to represent contributions from states not explicitly considered. The optical potential is evaluated through the use of a pseudostate expansion. Solutions are obtained by a linear algebraic integral equation method. Results are presented for elastic scattering and total cross sections for initial $1s$, $2s$, and $2p$ states. All $1s \rightarrow n=2$, $1s \rightarrow n=3$, and $n=2 \rightarrow n=3$ excitation cross sections are computed. Particular attention is given to obtaining convergence of sums with respect to the total angular momenta. Analytic formulas are given for the energy dependence of the cross sections from least-squares fits. Effective collision strengths are determined by averaging over a thermal distribution of incident electron energies.

I. INTRODUCTION

In a previous paper[1] we have expressed the point of view that the most satisfactory approach to intermediate-energy electron-atom (and electron-ion) scattering available at present would involve incorporation of an optical potential into the equations resulting from a limited close-coupling expansion. One solves the close-coupling equations including all states with which one is explicitly concerned (the P set), and takes account approximately of the other channels available to the physical system, whether open or closed (the Q set) by including them in a complex, energy-dependent, nonlocal optical-potential matrix. In principle, such a procedure is exact in that an optical-potential matrix can be defined such that the correct S-matrix elements are obtained among the P channels; but, in practice, approximations have to be made. These are of both a formal and a computational nature: For example, we neglect exchange couplings between the channels in the Q set, and then evaluate the optical potential by means of an expansion in a finite pseudostate set. The results, while not perfect, are expected to be a significant improvement over the usual close-coupling procedure in which no account of the Q channels is taken at all.

The present paper extends our previous applications of this approach to electron-hydrogen scattering in several respects: Perhaps most importantly, we have calculated cross sections for $1s \rightarrow n=3$ and $n=2 \rightarrow n=3$ excitations. These transitions are significant in plasma physics and astrophysics, and rather little is known about the cross sections for these processes.[2] (Some existing studies are discussed below.) It is characteristic of the $n=2 \rightarrow n=3$ transitions that a very large number of angular momenta contribute. We have tried here to obtain results which are converged in this respect. Our methods for doing this will be described below, in Sec. II. In addition, we give elastic scattering and total cross sections for the $1s$, $2s$, and $2p$ states. Comparisons with other calculations and with experiment are made where possible. Finally, we use our values for excitation cross sections, supplemented in some cases with results of previous variational calculations[3] to derive effective collision strengths for all the transitions considered. Rate coefficients are easily determined from the effective collision strength.

In contrast with $1s \rightarrow n=2$ transitions which have been extensively studied, there are relatively few investigations of $1s \rightarrow n=3$ and $n=2 \rightarrow n=3$ transitions. We note the existence of some unitarized Born,[4,5] distorted-wave,[6] Glauber,[7,8] and multichannel eikonal calculations,[9] but we will consider only close-coupling calculations in any detail here. The first such calculation which included $n=3$ states was performed by Burke, Ormonde, and Whittaker.[10] This work was restricted to energies in the neighborhood of the $n=3$ threshold. Six-state calculations over a large energy range were reported by Van den Ree,[11] but these are apparently not converged in regard to angular momenta. Such calculations do not make any allowance for additional channels. Hata, Morgan, and McDowell[12] use an algebraic variational method[13] in a calculation employing a basis of up to 18 states, including all $n=1$, 2, and 3 states exactly plus the $4f$; and eleven pseudostates (4 of s type, three of p type, 2 of d, 1 of f, and 1 of g). This is the basis used in Refs. 1 and 13 (7 s states, 5 p, 3 d, 2 f, and 1 g) and this is also the basis used in the present calculation in the construction of the optical potential. Their results were confined to energies between the $n=3$ and $n=4$ thresholds. [However, extensive calculations by one of us (J.C.) with the same basis have not confirmed the existence of a ^3S shape resonance above the $n=3$ threshold which they reported.]

The algebraic variational calculations become quite cumbersome at higher energies where high L values become important and in practice require supplementation

 ©1987 The American Physical Society

by some other method for L greater than a fairly modest value in the range of 3–5. One of us has recently reported calculations of elastic scattering in the $1s$ state and $1s \rightarrow n=2$ transitions in the 12–54-eV range of incident energies using the algebraic variational method with an 11-state basis (this does not include the $n=3$ states).[3] Partial-wave cross sections for $L \geq 6$ were obtained from the unitarized Born approximation with exchange. This procedure leads to an overestimate of the $2p$ excitation cross section at 54 eV.[14]

Edmunds, McDowell, and Morgan[15] have studied excitation of states including $n=4$ at two energies (35 and 54 eV) using close-coupling calculations. More recently, these calculations have been repeated and improved by Whelan, McDowell, and Edmunds[16] (whose results are restricted to transitions through $n=3$). However, both papers either neglect exchange entirely or incorporate it only through a local exchange potential. It is not clear at this time that exchange is negligible at these energies or that a local potential gives a satisfactory representation of exchange; however, their results are the most comprehensive in existence prior to the present calculation and detailed comparisons with their work will be made subsequently in this paper. We have benefited from their emphasis on the importance of high L contributions, particularly in regard to $n=2 \rightarrow n=3$ excitations.

McCarthy and Stelbovics[17] have reported a six-state coupled-channel optical-potential calculation at the single energy of 54 eV. (Other calculations by these authors and their collaborators have considered three states explicitly[18].) These calculations are conceptually similar to ours, but are carried out in a very different way in which coupled integral equations for T-matrix elements are solved in a momentum representation.[19] They report cross sections for $1s$ to $n=2$ and $n=3$ states only.

II. METHOD

Most of the work reported here is based on the optical-potential approach described in Ref. 1. The same basis of pseudostates employed in that paper is also used here. The coupled integro-differential equations were solved by a linear algebraic integral equation method. The algorithm employed has been described elsewhere.[20]

The coupled equations, including exchange and the optical potential were solved for values of the total angular momentum $L \leq L_1$. The value of L_1 varied with incident energy from 17 at $k^2=1.44$ to 35 at $k^2=7.35$. In a second range $L_1 \leq L \leq L_2$, exchange and the optical potential were dropped. ($L_2=48$ except for $k^2=0.91$, where $L_1=L_2=26$.) For $L > L_2$, inelastic cross sections were extrapolated, assuming that for a given transition

$$\frac{\sigma_{L+1}}{\sigma_L} = f(k^2) , \tag{1}$$

where f is independent of L. We then have

$$\sum_{L_2+1}^{\infty} \sigma_L \approx \frac{f\sigma_{L2}}{1-f} . \tag{2}$$

The quantity f was obtained from the values of σ_L for L close to L_2

This procedure is, obviously, rather crude. It is based on the assumption that for sufficiently large L ($\geq L_2$), partial cross sections decrease exponentially with L. This can easily be justified in a semiclassical treatment of the collision process for large values of the impact parameter. Equation (1) ignores, however, an L-dependent prefactor in front of the exponential. More importantly, Eq. (1) cannot be applied to processes such as $2s \rightarrow 2p$ transitions in which there is a change of state with no transfer of energy. In fact, the sum over angular momenta of the partial cross sections for transitions connected by a dipole matrix element in which there is no change of energy must diverge—the integrated cross section for $2s \rightleftarrows 2p$ transition is not finite. This is easily seen directly from the reactance matrix elements given analytically for large L by Kingston, Fon, and Burke,[21] which are proportional to $1/L$.

It follows from this that a total cross section for scattering in the $2s$ or $2p$ states cannot be defined. The total cross section is defined only for the $1s$ state, and exists because this state is not degenerate. In our tables, we give the total cross section for all transitions from the $2s$ and $2p$ states to final states other than $n=2$. This quantity is finite.

The extrapolation of the $2s$ and $2p$ elastic cross sections, which are finite, must take account of the dominant $2s \rightleftarrows 2p$ scattering. In these cases, it follows from the work of Kingston, Fon, and Burke, that the angular momentum weighted partial cross section σ_L decreases with L as

$$\sigma(L) = \text{const}/L^3 . \tag{3}$$

This form was used to extrapolate the elastic cross sections to convergence. The constant in Eq. (3) was determined empirically from the cross sections actually calculated for L close to L_2.

III. CROSS SECTIONS

Our results for the cross sections are given in Table I. In making this tabulation, we have, wherever possible, used results from variational calculations such as those described in Ref. 3 for small angular momenta. At $k^2=0.91$, we have been able to make variational calculations for $0 \leq L \leq 3$ and both conventional and unconventional parity using a rather large basis of 11 s states, 9 p states, 5 d, 2 f, and 1 g, including exactly all $n=3$ and $n=4$ states. These calculations will be described in more detail in a future report concerned with resonances between the $n=3$ and $n=4$ thresholds. The cross sections quoted in Table I combine the results of these variational calculations with optical-potential results for $4 \leq L \leq 26$.

For higher energies, variational calculations are available only using a smaller, 11-state basis set, as described in Ref. 3. These calculations cover angular momentum

TABLE I. Cross sections (units of πa_0^2) for several processes.

k_1^2	0.91	1.44	1.96	2.25	2.57	4.00	5.50	7.35
				Elastic				
$1s$	5.756	3.430	2.340	1.965	1.664	0.922	0.636	0.441
$2s$	207.7	63.32	38.42	30.89	25.37	13.80	9.196	6.430
$2p$	214.8	57.15	33.20	26.32	21.13	10.92	7.166	4.973
				$1s \rightarrow n=2$ excitations				
$1s \rightarrow 2s$	0.167	0.100	0.090	0.085	0.080	0.062	0.043	0.040
$1s \rightarrow 2p$	0.359	0.551	0.680	0.688	0.705	0.746	0.709	0.624
				$1s \rightarrow n=3$ excitations				
$1s \rightarrow 3s$	0.036	0.039	0.0179	0.0146	0.0123	0.0086	0.0072	0.0065
$1s \rightarrow 3p$	0.063	0.105	0.085	0.088	0.095	0.110	0.110	0.102
$1s \rightarrow 3d$	0.033	0.053	0.043	0.036	0.034	0.023	0.0158	0.0108
				$2s \rightarrow n=3$ excitations				
$2s \rightarrow 3s$	7.015	3.778	2.759	2.459	2.182	1.374	0.959	0.704
$2s \rightarrow 3p$	11.539	7.391	9.134	9.265	9.083	7.795	6.661	5.237
$2s \rightarrow 3d$	8.014	11.24	10.32	9.223	8.138	5.102	3.606	2.386
				$2p \rightarrow n=3$ excitations				
$2p \rightarrow 3s$	2.982	0.645	0.516	0.476	0.429	0.303	0.243	0.186
$2p \rightarrow 3p$	10.048	4.984	3.141	2.679	2.344	1.550	1.128	0.824
$2p \rightarrow 3d$	13.429	15.28	19.37	19.80	19.54	16.36	13.49	10.56
				$1s$ Total				
$1s$	6.416	4.741	4.054	3.866	3.673	2.933	2.484	1.972
				Total $n=2$ to all states except $n=2$				
$2s \rightarrow n \neq 2$	27.50	53.98	44.79	39.32	35.31	23.73	18.10	12.57
$2p \rightarrow n \neq 2$	27.14	50.15	48.00	45.09	41.87	31.10	23.37	17.24

$0 \leq L \leq 3$, and give results for $n=1$ and $n=2$ elastic and total cross sections plus $1s \rightarrow n=2$ and the $2s \rightleftarrows 2p$ transition. Partial cross sections from this work were incorporated in the $1s$ elastic, $1s \rightarrow 2s$, and $1s \rightarrow 2p$ entries in Table I.

These results can be compared with a series of close-coupling calculations reported by Edmunds, McDowell and Morgan[15] and Whelan, McDowell, and Edmunds[16] for incident energies including $k^2=2.57$ and 4.0. They present $1s \rightarrow n=2$ and $n=3$ and $n=2 \rightarrow n=3$ excitation cross sections from models containing differing numbers of pseudostates and exact states. Unfortunately, none of the calculations includes exchange exactly. Moreover, the results from their different models differ among themselves very substantially. For example, the different values they give for the $2p \rightarrow 3d$ cross section at $k^2=2.57$ range from $\sigma=15(\pi a_0^2)$ to $24\pi a_0^2$, a difference of about 40%. Our cross sections are smaller than theirs for all transitions except $2s \rightarrow 3s$. Our results are closest to the model they label "123NX7PS" at 54 eV and to the model "123NX6PS" at 35 eV. The degree of agreement is markedly better at 54 eV (within 10%, except for $1s \rightarrow 3s$ and $1s \rightarrow 3p$ transitions) than at 35 eV (8 out of 11 transitions differ by more than 10%). It is plausible that neglect of exchange in the work of Refs. 15 and 16 is a major contributor to the discrepancy since the effect of exchange should decrease with increasing energy, and our calculations show that exchange is not negligible at either energy. For example, in the case of the $1s \rightarrow 3s$ transition which shows the worst discrepancy (nearly 40% at 35 eV and 33% at 54 eV), we find that the ratio of singlet to triplet partial cross sections summed over all L is 0.70 at 35 eV and 0.55 at 54 eV. The expected ratio is 0.33 if exchange can be neglected. We will now discuss the cross sections as they are listed in Table I.

1s elastic. The results quoted in Table I are essentially the same as those given in Ref. 3. There are no direct experimental measurements of this quantity, of which we are aware, in the energy range of interest here. There are some measurements of elastic differential cross sections. De Heer, McDowell, and Wagenaar[22] obtained an integrated elastic cross section by integrating measured differential cross sections over angles. There may be some uncertainty in the results because an extrapolation has to be made at forward angles which are not included in the experimental measurements. Their results indicate clearly that at 50 and 100 eV our calculated $1s$ elastic scattering cross sections are significantly too small (Ref. 21 gives $\sigma_{el}=1.22\pi a_0^2$ at 50 eV and $0.597\pi a_0^2$ at 100 eV). The most probable cause of this discrepancy is that the pseudostate basis we use to evaluate the optical potential becomes progressively less adequate as the incident energy increases.

$n=2$ elastic. Our results for the elastic scattering cross sections from the $2s$ and $2p$ states are shown in Fig. 1. These cross sections are obviously very similar both in shape and magnitude. There are no experimental data at all. These cross sections are quite difficult to calculate because of the large contributions from higher angular momentum states. From the theoretical point of view, there is rather good agreement between the partial cross sections calculated using the variational approach of Ref. 3 for small angular momenta and those found from the optical-potential method. Further, the variational results, as far as they go, do not depend strongly

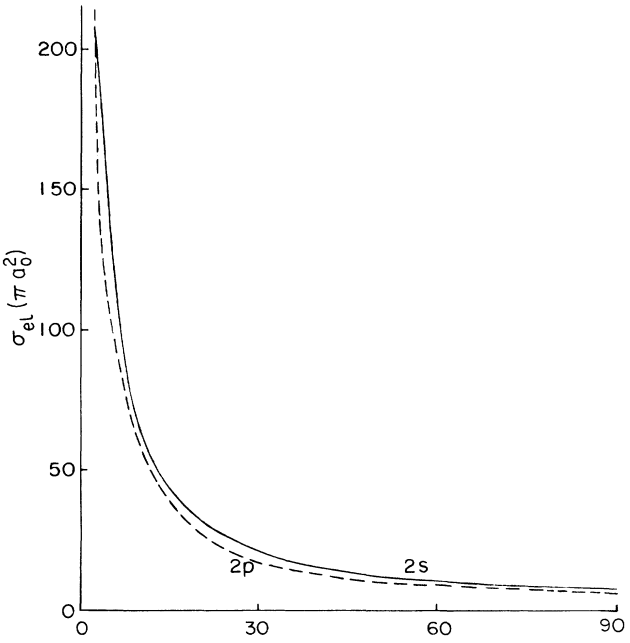

FIG. 1. Elastic cross sections (units of πa_0^2) for scattering from the $2s$ (solid line) and the $2p$ (dashed line) state. The energy scale refers to the energy of an electron incident on a hydrogen atom in one of the $n=2$ states (thus the energies are 10 eV less than those listed in Table I).

on the basis set employed. This supports a feeling of some confidence in the results, but in the total absence of experimental data or of calculations of a comparable level, it is impossible to make any quantitative estimate of accuracy.

Ho and Chan obtained $\sigma_{2s,el}=4162\pi a_0^2/105k^2$ from Born and Glauber calculations.[23] This expression describes their results for incident energies greater than 20 eV. This is a factor of 17 larger than the $1s$ elastic cross section, calculated in the same way in the high-energy limit. Our values for both the $1s$ and $2s$ states are somewhat larger than those of Ho and Chan; the ratio to the $1s$ cross section is about 14.5 at $k^2=5.50$ if the difference in the channel energies is neglected and is about 12 if this is taken into account. The ratio of geometric cross sections for $2s$ and $1s$ states $(\langle r\rangle_{2s}^2/\langle r\rangle_{1s}^2)$ is 16.

$1s\rightarrow n=2$ excitations. Limitations of space and scope do not permit us to review the vast theoretical literature on these processes here. Experimental information is quite sparse, and has not changed significantly since Ref.

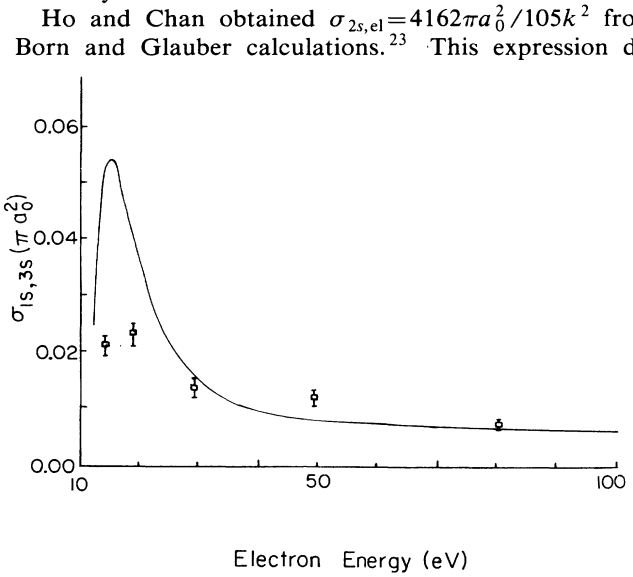

FIG. 2. Cross sections (units of πa_0^2) for the $1s\rightarrow 3s$ transition for incident electron energies up to 100 eV. Experimental points are from Ref. 22.

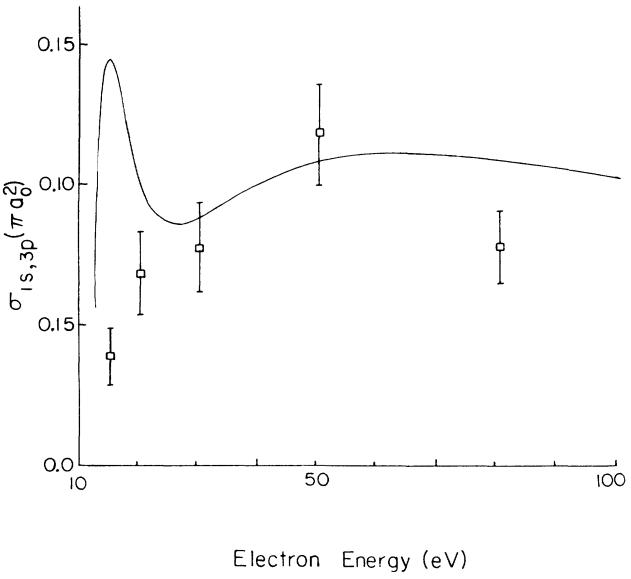

FIG. 3. Similar to Fig. for the $1s\rightarrow 3p$ transition.

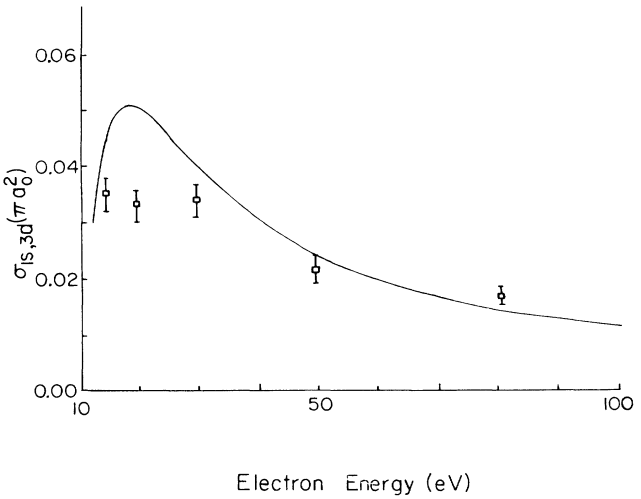

FIG. 4. Similar to Fig. 1 for the $1s\rightarrow 3d$ transition.

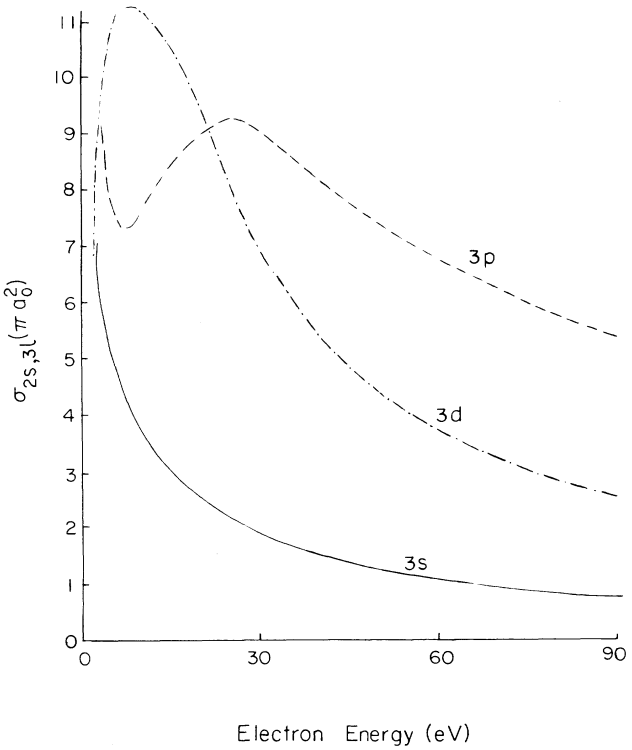

FIG. 5. Cross section (units of πa_0^2) for $2s$ to the $3s$ state (solid line), $3p$ (dashed line), and $3d$ (dashed-dotted line). The energy scale refers to the energy of an electron incident on a hydrogen atom in an $n=2$ state.

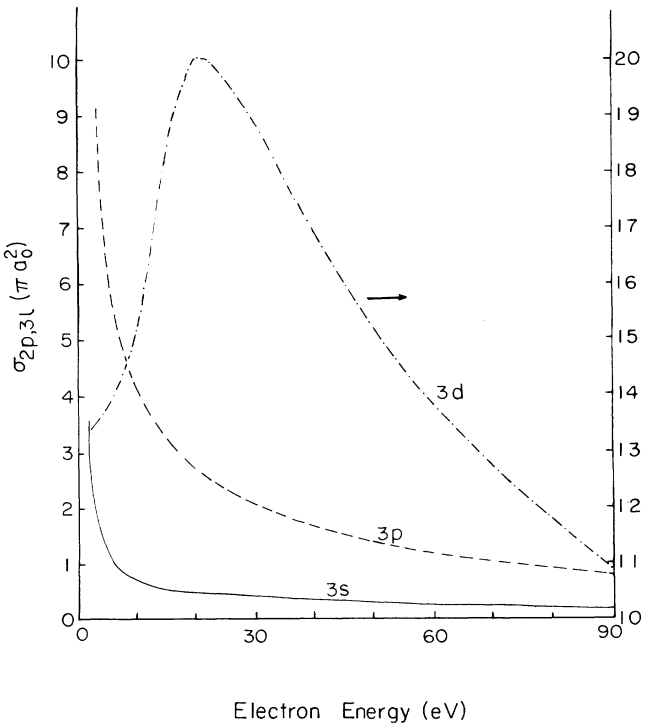

FIG. 6. Similar to Fig. 5 for the $2p \rightarrow n=3$ transitions. The $2p \rightarrow 3d$ transition refers to the right-hand scale.

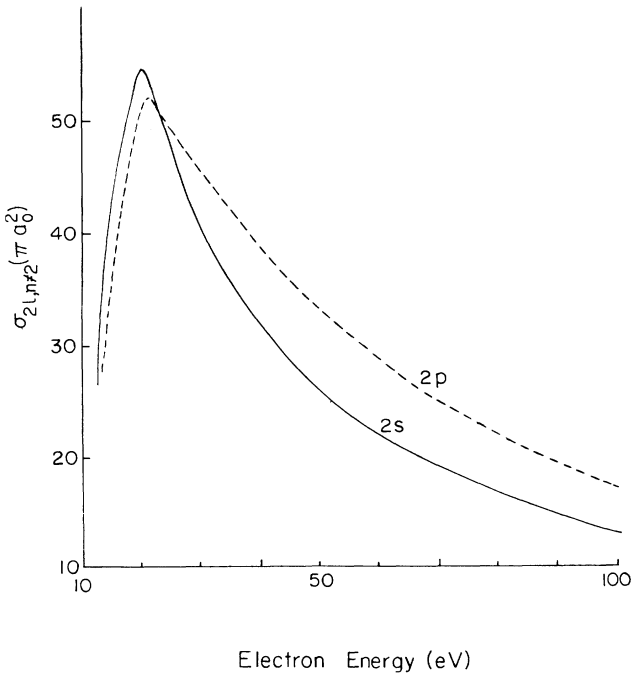

FIG. 7. Cross sections for transitions from the $2s$ (solid line) and $2p$ (dashed line) states to all states other than $n=2$.

2 was written. We believe that the present calculation of the $2p$ excitation cross section may be preferable on theoretical grounds to that presented in Ref. 3. The reason is that a large portion of this excitation comes from relatively high angular momentum states which were (inadequately) included in Ref. 3 using a unitarized Born approximation. This overestimates the high L contribution. The present approach should be more accurate. The cross section is reduced by about 12% at 54 eV, but we note that this reduction brings the theory into conflict with the "absolute" measurement of Willi-

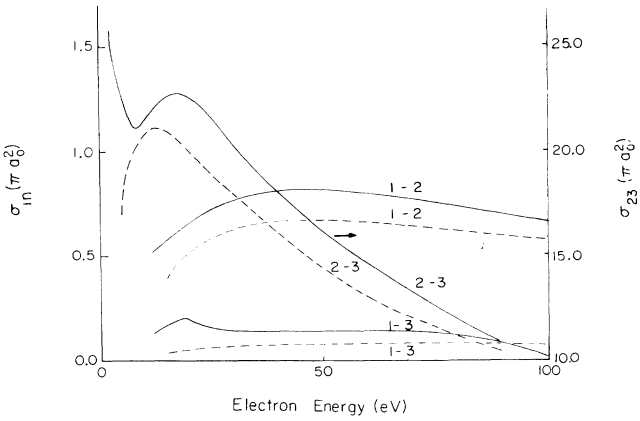

FIG. 8. Combined cross sections from our work (solid line) for $n=1$ to $n=2$ and $n=3$ (left-hand scale) and for $n=2$ to $n=3$ transitions (right-hand scale) are compared with the results of the semiempirical formula of Ref. 27.

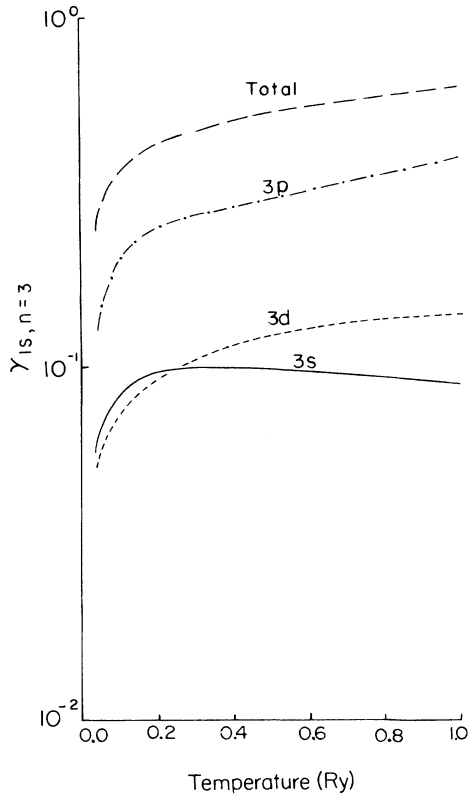

FIG. 9. Effective collision strengths for $1s$ to $n=3$ transitions ($3s$, solid line; $3p$, dashed-dotted line; $3d$, short-dash line; total $n=3$, long-dash line).

ams at this energy (0.89 ± 0.08)[24] Recently, Van Wyngaarden and Walters have argued that Williams's result might be wrong, and have urged repetition of the experiment.[14] We concur.

The $1s\rightarrow 2s$ cross section does not contain such large contributions from high angular momenta as does the $2p$ (because the $1s\rightarrow 2s$ transition potential is of short range). In this case, we believe that the results presented in Ref. 3 are as satisfactory as those given here (and are given for many more energies).

$1s\rightarrow n=3$ excitation. This work presents the first close-coupling calculation of $1s\rightarrow n=3$ transitions at most of the energies considered here. As this is a relatively unexplored topic at the present time, we present a detailed comparison between our results and the most recently reported experiment.[25] Our calculated cross sections for $1s\rightarrow 3s$, $1s\rightarrow 3p$, and $1s\rightarrow 3p$ excitations are shown in Figs. 2, 3, and 4 (for this purpose we have used the functional fits described below), respectively, where they are compared with the observations of Mahan, Gallagher, and Smith.[25] The agreement with experiment is quite reasonably good for 35 eV and higher. At lower energies the calculated values are larger than experimental ones for each case. We do not know whether this disagreement indicates a breakdown of the optical-potential approach near the ionization threshold, or whether there is an experimental problem in this region.

$n=2$ excitations. Our cross sections for $2s\rightarrow n=3$

TABLE II. Fitting coefficients for the collision strength [see Eqs. (7) and (8)]. Numbers in square brackets indicate powers of 10.

	$1s\rightarrow 2p$	$1s\rightarrow 3s$	$1s\rightarrow 3p$	$1s\rightarrow 3d$	$2s\rightarrow 3s$	$2s\rightarrow 3p$	$2s\rightarrow 3d$	$2p\rightarrow 3s$	$2p\rightarrow 3p$	$2p\rightarrow 3d$
a_0	8.9487[−1]	1.7628[−1]	3.9726[−1]	1.356[−1]	1.0632[+1]	−1.6889[+1]	3.470 942[+1]	−1.4641[+0]	3.4923[+1]	1.1033[+1]
a_1	−2.292 325[+1]	−9.000 861[−1]	−4.059 31[+0]	2.877 572[−1]	−5.336 33[+1]	−7.194 569[+2]	−5.439 227[+1]	−9.247 584[+0]	−6.920 705 4[+1]	−2.514 359[+3]
a_2	6.694 490 7[+1]	2.099 075[+0]	6.494 722[+0]	−5.539 363[−1]	2.419 371[+2]	1.785 167[+4]	−2.083 216 4[+2]	2.741 334[+2]	−1.413 177 0[+3]	2.035 028 5[+4]
a_3	−7.695 646 1[+1]	−1.325 035[+0]	−5.289 257[−2]	1.859 47[−1]	−5.512 759[+2]	−2.016 992[+5]	0.0[+0]	−1.697 846 2[+3]	9.654 004 2[+3]	−7.361 311 34[+4]
a_4	3.338 132 4[+1]	0.0[+0]	−2.725 791[+0]	0.0[+0]	0.0[+0]	7.909 88[+5]	0.0[+0]	0.0[+0]	0.0[+0]	0.0[+0]
a_5	4.439 432[+0]	0.0[+0]	7.1191[−1]	0.0[+0]	0.0[+0]	2.504 8[+1]	0.0[+0]	2.3483[+0]	0.0[+0]	1.2023[+2]
E_0	0.75[+0]	0.8889[+0]	0.8889[+0]	0.8889[+0]	1.25[+0]	1.25[+0]	1.25[+0]	1.5[+0]	1.5[+0]	1.25[+0]
a	0.0[+0]	0.0[+0]	0.0[+0]	0.0[+0]	1.0556[+0]	2.844[+0]	−1.998 88[+0]	2.970 497 8[+0]	7.848 333[+0]	2.717 650 9[+0]
b	0.0[+0]	0.0[+0]	0.0[+0]	0.0[+0]	1.0914[+0]	5.116 81[−1]	4.093 12[+0]	−1.611 298 7[−1]	2.294 688 9[+0]	7.696 39[+0]
c	0.0[+0]	0.0[+0]	0.0[+0]	0.0[+0]	−5.1213[−2]	1.950 29[−1]	−1.144 41[−1]	2.606 037 1[−2]	−7.345 314 2[−2]	9.188 212 8[−1]

and $2p \rightarrow n=3$ transitions are shown in Figs. 5 and 6, respectively. The curves are drawn from the functional fits described below. There are no experimental data. Van den Ree has made six-state close coupling (including exchange) of these quantities, but he presents only graphical results. While the present calculations are far more comprehensive than any previous work, the dependence of the results on the basis sets, noted above in connection with the work of Edmunds *et al.*,[15] makes it impossible to give an estimate of the reliability of our values.

Total cross sections. Use of a complex optical potential makes it possible to obtain a total cross section which includes contributions from states not explicitly included in the close-coupling calculation. A total cross section is found from the imaginary part of the partial-wave scattering amplitude via the optical theorem. Our results for the total cross section from the $1s$ state are in good agreement with our previous results[26] at low energies, and are somewhat larger (and therefore improved) at higher energies. In the case of the $n=2$ states, it was pointed out earlier that it is necessary to subtract the $2s \rightleftarrows 2p$ contribution to obtain a finite result. We present in Fig. 7 our results for the cross section for transitions from the $2s$ and $2p$ states to all other states.

The cross sections for the superelastic transitions $2s \rightarrow 1s$ and $2p \rightarrow 1s$ can be inferred from the data presented in Table I by multiplying the numbers given there for the excitations $1s \rightarrow 2s$ and $1s \rightarrow 2p$ by $k^2/[(k^2-0.75)(2l+1)]$, where l is the angular momentum of the initial state and k^2 is the energy for an electron incident on the ground state. If the sum of the superelastic cross sections and that for transitions to the $n=3$ states are subtracted from the total for states $n \neq 2$, the result is the cross section for transitions to all states higher than $n=3$, including ionization. This is, in fact, a rather large number: For example at $k^2=2.57$ (referred to the $n=2$ states, this corresponds to 24.75 eV), we find for this quantity $15.79\pi a_0^2$ for the $2s$ state and $19.23\pi a_0^2$ for the $2p$ state.

IV. ANALYTIC FITS AND EFFECTIVE COLLISION STRENGTHS

The collision strength for the transition $i \rightarrow f$ is defined by

$$\Omega_{if}=k_i^2 g_i \sigma_{if}(k_i^2) , \tag{4}$$

where k_i^2 is the incident electron energy and g_i the degeneracy of the initial state i. Calculation of the rate coefficient q in a plasma of temperature T (in K) given by[27]

$$q=\frac{8.63\times 10^{-6}\gamma e^{-\Delta E/kT}}{\sqrt{T}g_i} \text{ cm}^3 \text{ sec}^{-1} , \tag{5}$$

where ΔE is the excitation energy, k the Boltzmann constant, and γ the effective collision strength,

$$\gamma=\frac{\mu e^{\mu}}{kT}\int_1^{\infty} e^{-\mu x}\Omega_{if}(x)dx ,$$
$$\mu=\Delta E/kT, \quad x=k_i^2/\Delta E , \tag{6}$$

is greatly facilitated by analytical fits to $\Omega_{if}(x)$, considered as a function of the dimensionless parameter x. For sufficiently large x, the Born approximation suggests the form

$$\Omega_{if}(x)=\sum_{j=0}^{n} a_j x^{-j}+a_{n+1}\ln x . \tag{7}$$

In fact, this was found to be quite satisfactory for all $x(\geq 1)$ for $i=1$ and $f=3$. For $i=1$ and $f=2$, an additional term, given in Ref. 2, has to be added to cover the range between the $n=2$ and $n=3$ thresholds. Also, in the case of $i=2$, a parabolic fit of the form

$$\Omega_{if}(x)=b_1+b_2 x+b_3 x^2 \tag{8}$$

was found to be more appropriate for small x. The various coefficients and the incident energy E_0, below which the parabolic fit is to be used, are presented in Table II. Except for the transition $2p \rightarrow 3s$, the constants a_0 and

TABLE III. Effective collision strengths.

kT (Ry)	$1s \rightarrow 2p$	$1s \rightarrow 3s$	$1s \rightarrow 3p$	$1s \rightarrow 3d$	$2s \rightarrow 3s$	$2s \rightarrow 3p$	$2s \rightarrow 3d$	$2p \rightarrow 3s$	$2p \rightarrow 3p$	$2p \rightarrow 3d$
0.04	0.397	0.0597	0.127	0.0524	2.372	3.843	3.074	2.808	10.676	14.231
0.05	0.397	0.0659	0.144	0.0572	2.439	3.923	3.341	2.803	10.824	15.003
0.10	0.445	0.0838	0.201	0.0733	2.755	4.402	4.643	2.784	11.540	19.150
0.15	0.527	0.0923	0.229	0.0840	3.045	4.978	5.886	2.778	12.218	23.770
0.20	0.619	0.0966	0.246	0.0924	3.309	5.644	7.067	2.786	12.858	28.833
0.25	0.715	0.0988	0.258	0.0992	3.551	6.383	8.184	2.806	13.461	34.264
0.30	0.812	0.0996	0.268	0.105	3.772	7.177	9.234	2.835	14.030	39.955
0.35	0.909	0.0997	0.276	0.110	3.975	8.008	10.215	2.873	14.565	45.806
0.40	1.006	0.0993	0.283	0.114	4.162	8.863	11.131	2.917	15.070	51.731
0.45	1.102	0.0987	0.291	0.118	4.336	9.732	11.984	2.965	15.547	57.664
0.50	1.197	0.0979	0.299	0.121	4.496	10.605	12.778	3.017	15.998	63.559
0.60	1.384	0.0960	0.315	0.127	4.786	12.341	14.209	3.126	16.832	75.110
0.70	1.567	0.0942	0.333	0.132	5.040	14.039	15.456	3.238	17.585	86.230
0.80	1.746	0.0925	0.351	0.136	5.265	15.684	16.551	3.350	18.269	96.859
0.90	1.921	0.0909	0.370	0.139	5.467	17.266	17.519	3.460	18.893	106.985
1.0	2.091	0.0895	0.390	0.141	5.649	18.785	18.380	3.567	19.466	116.622

a_{n+1}, with $n=4$, were constrained to have the values predicted by the Born approximation, and the rest were determined by least-squares fitting. As mentioned previously, these fits were used for some of the figures.

It is of some interest to compare the results of the present calculations as expressed through these fits with existing semiempirical formulas. Because so little accurate information is available for excitation cross sections other than $1s \rightarrow n=2$, workers in astrophysics and plasma physics who needed estimates of transition rates have had to rely on such formulas. We compare in Fig. 8 our results for $n=1$ to $n=2$, and $n=3$, and $n=2$ to $n=3$ total cross sections with the formula given by Vriens and Smeets.[28] (In the last case, we have taken $\sigma_{23}=\frac{1}{4}\sigma_{2s,\,n=3}+\frac{3}{4}\sigma_{2p,\,n=3}$.) It will be seen from the figures that the cross sections from the semiempirical formulas are always smaller than those we have calculated. Consider 54 eV as a typical energy. The estimate of Ref. 27 is too low for σ_{12} by 20%, for σ_{13} by 40%, and for σ_{23} by 11%. At low energies, the discrepancies are worse, about a factor of 2 for $n=2$ to $n=3$, and a factor of 3 for $1s$ to $n=3$. Hence, use of the present results will make a significant difference in calculations of rate coefficients or effective collision strengths.

Our results for the effective collision strengths can be expressed analytically in terms of the coefficients a_i and b_i as follows:

$$\gamma=\gamma_1+\gamma_2 , \tag{9a}$$

$$\gamma_1=\mu e^{\mu}(b_1 I-b_2 I'+b_3 I'') , \tag{9b}$$

$$I(\mu)=\frac{e^{-\mu}-e^{-\mu x_0}}{\mu} , \tag{9c}$$

$$\gamma_2=e^{\mu}\left[\sum_{i=0}^{n}\mu a_i x_0^{-i+1}E_i(\mu x_0) + a_{n+1}[e^{-\mu x_0}\ln x_0+E_1(\mu x_0)]\right] , \tag{9d}$$

where the primes denote differentiations with respect to the argument, $x_0=E_0/\Delta E$ and E_i is an exponential integral,

$$E_i(\mu)=\int_1^{\infty}\frac{e^{-\mu x}}{x^i}dx . \tag{9e}$$

Effective collision strengths for various transitions in the range $0.04 \leq kT \leq 1$ Ry are given in Table III. The $1s \rightarrow 2p$ results (Table I) are somewhat smaller than the corresponding value reported earlier on the basis of an 11-state calculation (Ref. 3) as discussed above. In the case of the $1s \rightarrow 2s$ transition, we recommend use of the results of Ref. 3.

The effective collision strengths are shown graphically in Figs. 9–11. It will be observed that the $n=2$ to $n=3$ collision strengths are dominanted for the temperatures considered by transitions with a $3d$ final state. This is as expected for $2p$ to $3d$, but perhaps not so for $2s$ to $3d$.

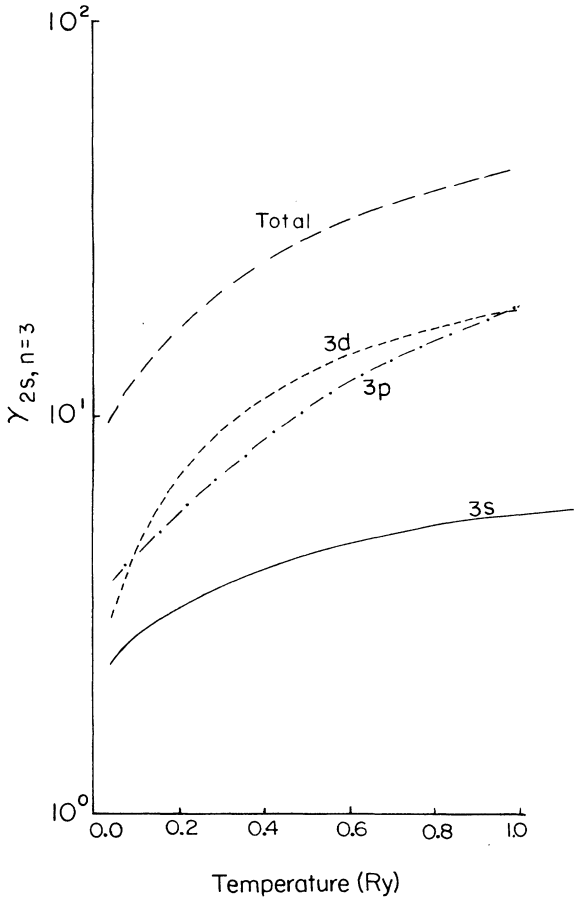

FIG. 10. Similar to Fig. 9 for $2s$ to $n=3$. Note that the energy scale refers to an electron incident on an atom in the $n=2$ state.

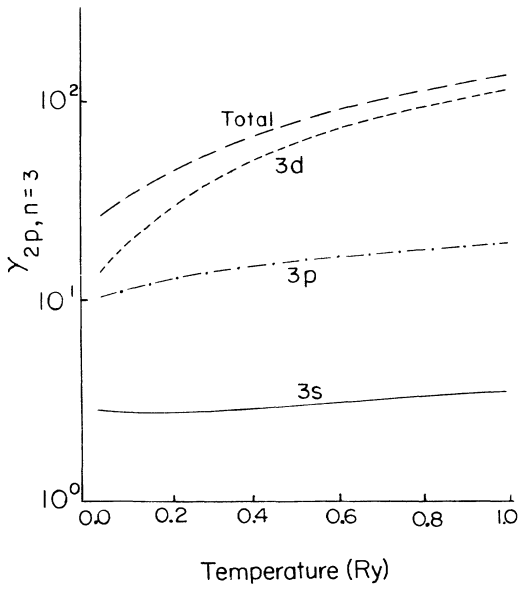

FIG. 11. Similar to Fig. 10 for $2p$ to $n=3$.

V. CONCLUSIONS

We have calculated cross sections for $1s$ to $n=2$ and $n=3$ and $n=2$ to $n=3$ excitations; elastic scattering cross sections in the $1s$, $2s$, and $2p$ states, plus total cross sections insofar as these exist. A six-state close-coupling expansion was employed, and a complex optical potential was included to incorporate effects of channels not considered explicitly. Where available, results for some partial waves from variational calculations were included. Analytic representations of the collision strengths have been obtained for the convenience of potential users of these data. Quantities closely related to rate coefficients (effective collision strengths) have been obtained by averaging over a Maxwell distribution of incident energies. Substantial differences between the present results and existing semiempirical formulas have been found, particularly at low energy.

What is really lacking is an adequate evaluation of the accuracy of the theoretical methods employed through confrontation with experiment. This is particularly serious in the case of $n=2$ to $n=3$ transitions where the theoretical uncertainties are greatest. Some of these transitions—those with an initial $2s$ state—ought to be accessible to experiment. We urge that these fundamental problems not continue to be neglected by experimentalists.

ACKNOWLEDGMENT

This work was supported in part by the U.S. National Science Foundation under Grant No. PHY-8514639.

[1]J. Callaway and D. H. Oza, Phys. Rev. A **32**, 2628 (1985).
[2]J. Callaway and M. R. C. McDowell, Comments At. Mol. Phys. **31**, 19 (1983).
[3]J. Callaway, Phys. Rev. A **32**, 775 (1985).
[4]W. B. Somerville, Proc. Phys. Soc. London, Ser. A **82**, 446 (1963).
[5]C. T. Whelan, J. Phys. B **19**, 2343, (1986); **19**, 2355 (1986).
[6]R. F. Syms, M. R. C. McDowell, L. A. Morgan, V. P. Myerscough, J. Phys. B **8**, 2817 (1975).
[7]K. Bhadra and A. S. Gosh, Phys. Rev. Lett. **26**, 737 (1971).
[8]H. Tai, R. H. Bassel, E. Gerjuoy, and V. Franco, Phys. Rev. A **1**, 1819 (1970).
[9]M. R. Flannery and K. J. McCann, J. Phys. B **7**, L522 (1974).
[10]P. G. Burke, S. Ormonde, and W. Whittaker, Proc. Soc., London **92**, 319 (1967).
[11]J. Van den Ree, J. Phys. B **15**, 2245 (1982).
[12]J. Hata, L. A. Morgan, and M. R. C. McDowell, J. Phys. B **13**, 4453 (1980).
[13]J. Callaway, Phys. Rep. **45** 89 (1978).
[14]W. L. Van Wyngaarden and H. R. J. Walters, J. Phys. B **19**, L53 (1986).
[15]P. W. Edmunds, M. R. C. McDowell, and L. A. Morgan, J. Phys. B **16**, 2553 (1983).
[16]C. T. Whelan, M. R. C. McDowell, and P. W. Edmunds, J. Phys. B **20**, 1587 (1987).
[17]I. E. McCarthy and A. T. Stelbovics, J. Phys. B **16**, 1611 (1983).
[18]B. H. Bransden, I. E. McCarthy, J. D. Mitroy, and A. D. Stelbovics, Phys. Rev. A **32**, 166 (1985).
[19]I. E. McCarthy and A. T. Stelbovics, Phys. Rev. A **28**, 2693 (1983).
[20]D. H. Oza and J. Callaway, J. Comput. Phys. **68**, 89 (1987).
[21]A. E. Kingston, W. E. Fon, and P. G. Burke, J. Phys. B **9**, 605 (1976).
[22]F. J. de Heer, M. R. C. McDowell, and R. W. Wagenaar, J. Phys. B **10**, 1945 (1977).
[23]T. S. Ho and F. T. Chan, Phys. Rev. A **17**, 529 (1978).
[24]J. F. Williams, J. Phys. B **14**, 1197 (1981).
[25]A. H. Mahan, A. Gallagher, and S. J. Smith, Phys. Rev. A **13**, 156 (1976).
[26]J. Callaway and D. H. Oza, Phys. Rev. A **34**, 965 (1986).
[27]S. S. Tayal and A. E. Kingston, J. Phys. B **17**, 1383 (1984).
[28]L. Vriens and A. H. M. Smeets, Phys. Rev. A **22**, 940 (1980).